Atmospheric EHF Window Transparencies near 35, 90, 140, and 220 GHz

HANS J. LIEBE, SENIOR MEMBER, IEEE

Abstract—**Transparency of the four atmospheric extremely high frequency (EHF) window ranges located around 35, 90, 140, and 220 GHz is obscured by precipitation (rain, wet snow), by suspended particles (fog, cloud, haze, dust), and by water vapor. An assessment is made of the quantitative picture (i.e., models versus experiments and theory), upon which estimations for general radio path behavior can be based. Useful models are provided for calculating attenuation based upon measurable meteorological variables: rain rate, liquid water content, humidity, temperature, and pressure. Information currently available is not yet complete enough to provide accurate predictions under all climatological conditions. Emphasis is on recent advances in formulating the physical basis for modeling transparency and on a discussion of some of the principal remaining uncertainties.**

I. INTRODUCTION

New requirements for high data-rate communication links, for active and passive sensors, and in radio astronomy have kindled growing activity in the extremely high frequency (EHF) (30 to 300 GHz) region of the radio spectrum. Progress is spurred by available bandwidth and size reduction, and by advantages over infrared and optical systems in penetrating an opaque atmosphere. Nevertheless, atmospheric propagation limitations dominate most considerations in the advancement of applications—adverse weather causing attenuation by rain, wet snow, and fog and by water vapor, is of serious consequence to EHF system performance. In recent years, numerous research and measurement programs have been carried out to make these detrimental effects predictable. A wealth of material has been accumulated and was carefully reviewed [1]-[9]. Here we limit the discussion to attenuation in transparent portions of the EHF range, somewhat loosely defined by a transmission factor

$$\mathbf{T} = \exp(-0.2303A) \geq 0.01 \quad \text{or} \quad A \leq 20 \text{ dB}. \tag{1}$$

Expression (1) implies that at least one percent of the transmitted power can be received. The total radio path attenuation A in decibels is a measure of the energy extracted from a plane wave by the atmospheric propagation medium. For a given situation, attenuation A can be evaluated when the number of all types of absorbers and scatterers within a radio path is known. A specific attenuation α is introduced when the mean absorber density is constant along a path length L, yielding

$$\alpha = A/L \qquad \text{dB/km}. \tag{2}$$

This mini-review was invited by the IEEE Wave Propagation Standards Committee.

Manuscript received March 24, 1982; revised June 26, 1982. This work was supported in part by the U.S. Army Research Office under Contract ARO 51-81/6-82.

The author is with the National Telecommunications and Information Administration, Institute for Telecommunication Sciences S3, Boulder, CO 80303.

TABLE I
EHF WINDOW FREQUENCY RANGES OF THE ATMOSPHERE (SEE FIG. 1)

WINDOW ID	FREQUENCY RANGE f, GHz	CLEAR AIR ATTENUATION (Sea Level, 15°C, 50 RH) α, dB/km
W1	25 to 50	0.1 to 0.5
W2	70 to 115	0.5 to 2
W3	125 to 160	2 to 5
W4	200 to 250	5 to 10

In clear air one can expect relatively low values for α (i.e., useful lengths L for a given value of A) in four distinct frequency ranges (see Table I), for which the metaphor "window" is used. The frame for these windows is set up by molecular resonance absorption of H_2O (centered at 22, 183, and 325 GHz) and O_2 (centered at 60 and 119 GHz) as illustrated in Fig. 1 [10]. It appears that about 150 GHz of the EHF band are available for signal transmission. A closer look reveals that the windows are veiled by water vapor and suspended hydrometeors and darkened by precipitation.

Recently Crane [11], [1] compared all readily available clear air EHF window data with model calculations for a standard condition (sea level, 20°C, 7.5 g/m^3 H_2O). Attenuation α, within measurement uncertainty, was supported by about 130 data points from 26 references; and for a zenith path attenuation A_z, starting at standard sea level conditions, about 60 data points from 22 sources were available. He agrees with previous workers that an empirical correction is required to reconcile observations with H_2O line calculations and that information is missing to establish the physical basis for such a correction. This mini-review goes one step further in that it is assumed that a theoretical model modified by an empirical term [10] correctly renders the window attenuation dependences and is then reduced to power law expressions in terms of meteorological variables.

II. TRANSMISSION PRINCIPLES AND EHF CLIMATOLOGY

Analysis of **T** (1) is not trivial. The loss of plane wave power by the cumulative effects of all absorbers in a radio path of length L is tallied by the total attenuation

$$A = \int_0^L [\alpha_R(x) + \alpha_W(x) + \alpha_V(x) + \alpha_D(x)]\, dx \qquad \text{dB}. \tag{3}$$

where α is the specific attenuation of an air volume element over a path increment dx and the subscripts R, W, V, D designate the absorbers rain, suspended hydrometeors (fog, cloud, haze, water cluster), water vapor, and dry air, respectively.

The physical state of air at a point x along the path is identified by five basic meteorological parameters $p\theta v$, w, and R described

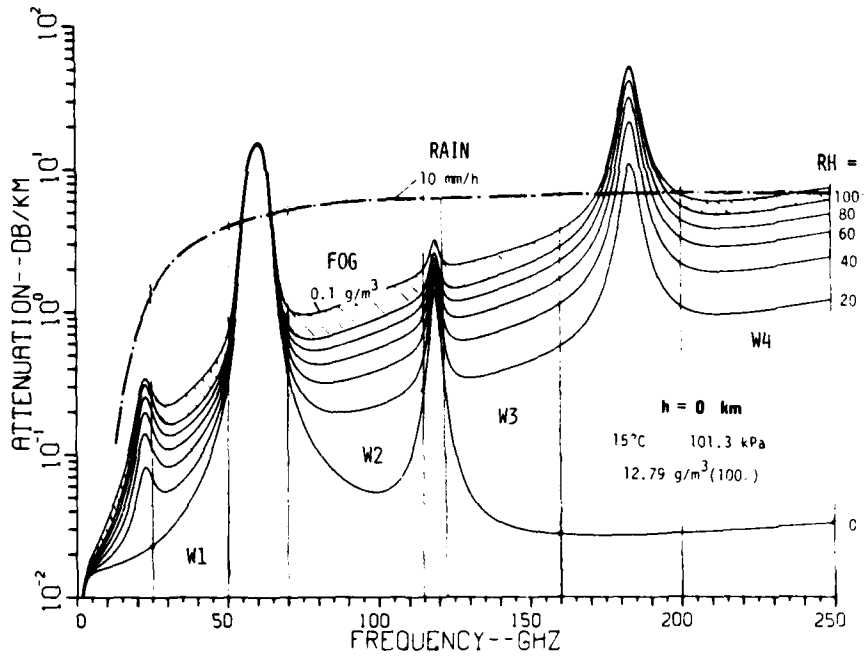

Fig. 1. Specific attenuation at sea level over the frequency range 1–250 GHz for various relative humidities (0 to 100 percent), including fog (0.1 g/m3) and rain (R = 10 mm/h).

and ranged below.

A. Moist air:

$$p(x) = (P - e) \quad \text{kPa}, \tag{4a}$$

dry air pressure where P is the barometric pressure;

$$\theta(x) = 300/T, \tag{4b}$$

relative inverse temperature (1.5 to 0.95 for T = 200 to 315 K);

$$v(x) = 7.219e\theta \quad \text{g/m}^3, \tag{4c}$$

water vapor concentration where e is the partial vapor pressure– or by

$$\text{RH}(x) = 41.51e/(\theta^5 \times 10^{(10-9.834\theta)}) \approx 29e\theta^{18} \leqslant 100 \text{ percent}, \tag{4d}$$

relative humidity ($\theta = \theta_1$ is the dew point at relative humidity (RH) = 100 percent).

Water vapor variability at sea level (p = 101 kPa, θ = 1.016 or 22°C) is typically

Dry	Normal	Humid	Saturated	
v = 1	10	17	20	g/m3
RH = 5	50	85	100	percent

B. Suspended hydrometeors are described by the liquid water concentration w, which relates approximately to optical (0.55 μm) visibility U (km) [4].

$$w(x) \approx 0.011/U^{1.7} \quad \text{g/m}^3. \tag{4e}$$

A schematic categorization can be made by

Cluster [21]	Haze	Fog [44]	Stratus	Convective Cloud	
$w = 10^{-3}$	10^{-2}	10^{-1}	1	5	g/m3
$U \cong 17$	1.1	0.27	0.07	0.03	km

C. Precipitation originates as a highly statistical event within clouds suspended in saturated air. Its vertical distribution is separated into two regions by the height of the 0°C isotherm, which can vary between ≈6 km and ground level depending on season and latitude. The lower part is mostly liquid drops, and the upper region consists of frozen particles with occasional supercooled droplet-loadings by strong updrafts.

Yearly statistics on local point rain rates $R(x_i)$ have proven useful in modeling rain-induced attenuation effects [13]–[18], [43], [45]. Rain rate can be related to the percent time t_R, a given value occurs over the period of an "average" year; the effective rain cell extent L_R/L; and the instantaneous suspended liquid water concentration,

$$w_R = mR(x) \quad \text{g/m}^3. \tag{4f}$$

In terms of these variables, a typical local rain may be classified as follows (horizontal path, L = 10 km):

Drizzle		Steady	Heavy	Downpour	Cloudburst	
R	= 1	5	20	100	250	mm/h
t_R	≃ 2	0.5	0.07	0.001	0.0001	percent/yr
L_R/L	≃ 1	1	0.7	0.35	0.2	
m	≃ 0.1	0.07	0.05	0.04	0.04	

The simple coefficient scheme reveals some fundamentals of rain that require consideration in attenuation models. Changes in the factor m indicate rain rate-dependent characteristics of drop size distributions. Widespread steady rain occurs more uniformly and favors small drop sizes (≤1 mm diameter) which stay in the air longer.[1] Heavy showers are more localized, favor larger drops and occur less frequently.

[1] Fall velocities in still air range between 1 and 9 m/s for drop diameters between 0.2 and 7 mm.

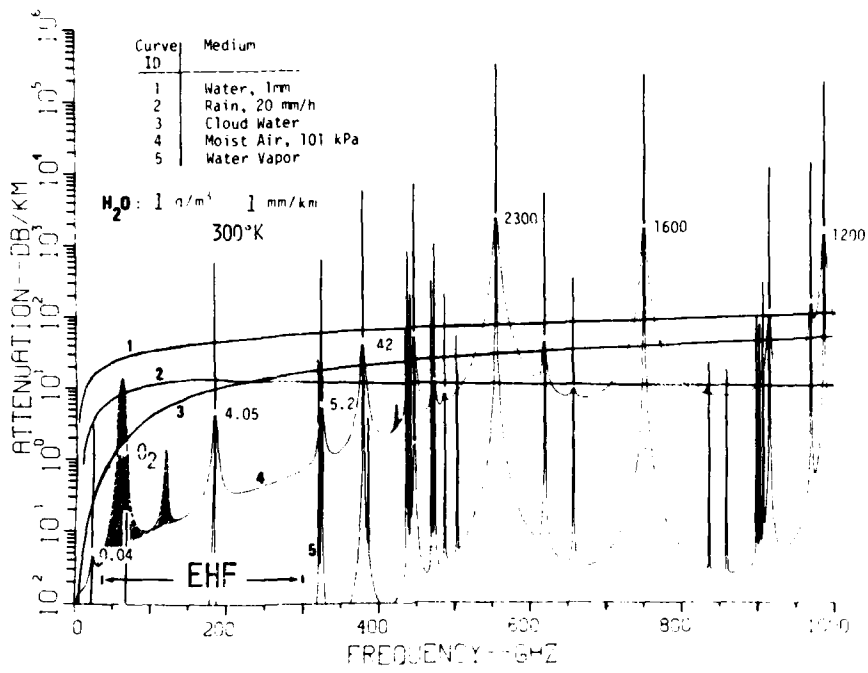

Fig. 2. Normalized (1 g/m^3, 300 K) specific H_2O attenuation over the frequency range 5-1000 GHz for five phase states: water 1), rain 2), suspended hydrometeors 3), moist air 4) (numbers shown indicate selected H_2O attenuation peaks), and pure water vapor 5) [10].

Three snow classes may be approximated:

Dry		Moist		Wet	
$R_S = 0.1$		1		5	mm/h
$T = -10$	−5		0		+5 °C,

where a snow-equivalent rate R_S can be obtained from a heated rain gauge.

Climatological extremes for locations in the continental U.S. span the following range.

	Rain (R)	Water Vapor (v)	Temperature (θ)
	Annual Rate	Greatest Monthly Concentration	Mean Annual Relative Temperature
Minimum	180 mm, Phoenix	6.5 g/m^3, Denver	1.042 (14.8°C), San Francisco
Maximum	1620 mm, New Orleans	21 g/m^3, Miami	0.984 (31.7°C), Phoenix

At this point it is assumed that for a given radio path the geometric, climatological, and temporal statistics of the meteorological measurables (4) are available and that models and/or theories exist to correlate ($p\theta v + w + R$) combinations with A (3).

III. SPECIFIC ATTENUATION

In the EHF window ranges, it is possible to formulate simplified expressions for the specific attenuation α. Water in both liquid and vapor states obscures window transparencies for ground-based system applications. Frequency dependence and magnitude of H_2O attenuation is distinctly different for the same absorber thickness 1 mm (later see (13)) in water, rain, suspended droplet, moist air, and pure water vapor forms, as depicted in Fig. 2. The three atmospheric phase states lie somewhat between the extremes of continuum-type water (curve 1) and resonance-type vapor (curve 5) spectra. Parameterization of specific attenuation on the basis of (4) is treated in the following manner.

- Rain attenuation can be fitted to [13]

$$\alpha_R = aR^x \quad \text{dB/km}, \tag{5}$$

bypassing elaborate, lengthy Mie calculations which require drop shape, size distributions, and the complex dielectric constant of water [12]-[14]. Drop diameters and EHF wavelengths (0.1-5 mm) are roughly comparable, thus causing appreciable attenuation via resonance (Mie) scattering. The frequency-dependent coefficient a and exponent x (Table II) were calculated using drop-size spectra of Laws and Parsons.

Considerable effort has been made to measure and to describe rain attenuation. Rain cell extent L_R and path-averaged rain rate $\bar{R}$ are obtained from cumulative distributions of attenuation A or point rate R at many locations over long time periods, preferably several years. Statistical estimation methods and models for the quantity $(\alpha L)_R$ are discussed in detail by Ippolito [2], [3]. A large bibliography exists on the topic of computing α_R distributions for general radio paths on the basis of point rainfall observations. More recent models are those by Lin or Dutton *et al.* (U. S.) [15], [43]; Morita (Asia) [17]; Misme-Waldteufel (Europe) [42]; and Crane (worldwide) [18]. A typical requirement in system design is to know for a given location the par-

TABLE II
COEFFICIENTS a–d AND EXPONENTS x, y FOR CALCULATING SPECIFIC ATTENUATION α (3) IN THE FOUR EHF WINDOW RANGES (SEE FIG. 1)

EHF Window	Frequency f	Rain (Low) $R \leq 50$ a	x	Rain (High) R = 25–200 a	x	Snow a_S	x_S	Haze, Fog, Cloud b	y	Water Vapor c	c'	Dry Air d
	GHz											
		Reference		[13]		[19], [20]		[10]				
											×10⁻²	×10⁻²
	25	0.11	1.08	0.14	1.02	0.05 dry	1.7	0.30	7.0	0.017	0.44	0.022
W1	35	0.24	1.02	0.34	0.91	0.25 moist	.9	0.59	6.4	0.010	0.27	0.035
	50	0.48	0.91	0.66	0.82	0.5 wet	.6	1.17	5.9	0.017	0.44	0.270
	70	0.80	0.81	0.86	0.79	0.3 dry	1.5	2.20	4.8	0.032	0.83	0.336
W2	90	1.03	0.76	0.94	0.78	1.4 moist	1	3.45	3.6	0.049	1.27	0.054
	115	1.12	0.73	0.98	0.77	2.5 wet	7	5.17	2.2	0.082	2.11	0.230
										[30], [10]		
	120	1.16	0.72	0.99	0.77	0.5 dry	1.3	5.53	1.9	0.087	2.22	0.800
W3	140	1.25	0.71	1.00	0.77	2.5 moist	1	6.95	0.9	0.116	2.98	0.029
	160	1.30	0.70	1.01	0.76	4.0 wet	.9	8.36	−0.1	0.190	4.88	0.024
	200	1.48	0.66	1.06	0.76	0.7 dry	1	10.9	−1.6	0.28	7.14	0.024
W4	220	1.47	0.66	1.05	0.76	3.0 moist	1	12.1	−2.1	0.24	6.20	0.026
	250	1.47	0.66	1.03	0.76	5.2 wet	1	13.4	−2.8	0.30	7.63	0.029

AVERAGE OF REPORTED FIELD DATA

		a	Reference	a_S (moist)	a_S (wet)	Reference	b	Reference	c	Reference
W1	35			0.2	0.4(1)	[7]	0.4(1)	[7]	0.009(3)	[7], [11]
W2	90	0.9(1)*	[7]	1.8(5)	3.0(6)	[7], [19]	4.5(5)	[7]	0.04(2)	[4], [7], [11]
W3	140	1.1(3)	[7]	3.0(8)	5(1)	[7], [19]	6(1)	[7]	0.13(5)	[4], [7], [11]
W4	220	1.5(8)	[20]	3.5(10)	6(1)	[20]	10(2)	[20]	0.3(1)	[4], [20], [11]

* Digits in parentheses give the standard devaition from the mean in terms of the final listed digits.
a (db/km)/(mm/h).
b, c (dB/km)/(g/m³).
c' (dB/km)/percent.
d (dB/km)/kPa.

ticular rain rate (attenuation) that is not exceeded by more than 0.01 percent (1 h) of the time over a year's period. Costly design decisions hinge on this rain information. For example, the 1 h/yr rain rate expectation in the continental U. S. has extremes between 7 (Arizona desert) and 115 mm/h (south Florida). Rain attenuation statistics for a terrestrial path in mid-U. S. are shown in Fig. 3, as calculated with Crane's prediction model (zone D_2) [18], extended in frequency beyond 100 GHz by results from [13].

- Snow is difficult to model since it is highly inhomogeneous. Around 0°C, flakes carry varying amounts of free water. During a snow storm in the northeast of the U. S., the equivalent liquid concentration was found to vary between 0.2 and 0.8 g/cm³ [19]. Data on A_S and R_S are few and have been fitted to (5). The resulting parameters a_S and x_S (see Table II) yield only first estimates.
- Suspended hydrometeor attenuation is formulated by

$$\alpha_W = bw\theta^y \quad \text{dB/km}. \tag{6}$$

The calculation of α_W is based upon the Rayleigh absorption approximation of Mie scattering [14]. Diameters of suspended particles are below 0.1 mm and any detailed drop-size distribution reduces to a liquid water concentration w. The Debye model for the complex dielectric constant of water enters into the computation of the parameters b and y (see Table II). Unlike rain, a strong temperature dependence can be noticed. Neutral water clusters (five to 30 molecules), whose existence is not directly confirmed, would add very little to α_W since even relatively high predicted number densities ($\leq 10^{13}$ cm^{-3}) [21] only yield low concentrations, $w < 10^{-3}$ g/m³.

Interrelations between the "EHF weather" parameters (4) are not treated, although H_2O is an incessantly phase-changing agent in the hydrological cycle between condensation sites and the atmospheric water vapor content. For example, at high relative humidities (RH > 90 percent), a small portion of water vapor is converted into submicron droplets by water uptake of aerosol particles leading to the formation of haze ($w < 10^{-2}$ g/m³) [22]. Heavy fog and clouds can exceed 0.1 g/m³, causing appreciable specific attenuation α_W. Cloud attenuation in W3 and W4 can rival rain attenuation depending upon the extent L_W (0.1 to 3 km) of the absorption cell.

- Water vapor attenuation is modeled by

$$\alpha_V = c(p/101)v\theta^y \approx c'(p/101)\,\mathrm{RH}/\theta^{1.7} \quad \text{dB/km} \tag{7}$$

where y = 1.8, 2.4, and 3.2 in W1, W2, and W3, 4, respectively. The attenuation depends on absolute (v) humidity limited by RH (note the steep temperature dependence (4d)), and varying greatly with both time and location [23]. On a hot (35°C) summer day, the vapor concentration can reach $v \cong 40$ g/m³ at RH > 90 percent.

The scale factor c has its origin in the absorption lines of H_2O vapor. In principle, it can be evaluated from a line-by-line summation of all line features, each contributing at a given frequency

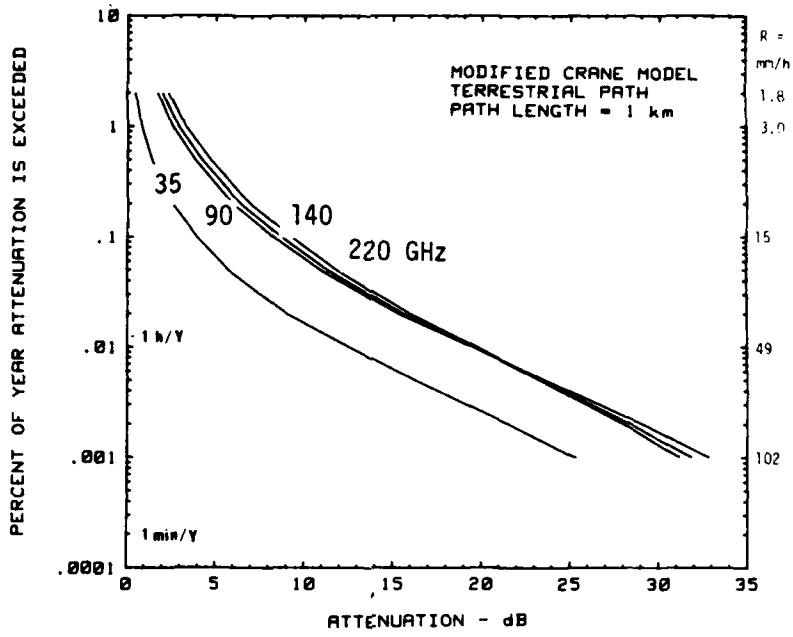

Fig. 3. EHF window rain attenuation predictions for a terrestrial (h = 0 km) path of 1 km length using for a mid-U.S.A. region the Crane model [18].

TABLE III
WATER VAPOR CONTINUUM: COEFFICIENTS DUE TO LINES [27] ABOVE 1 THZ

	Equation	k	x	y	z	Line Shape		
THEORY	(8a)	0.0014	1.0	2	2.51	MGR	(GR) × f/ν_0	(Modified GR)
	(8b)	0.0064	1.05	1.4	2.05	VW	Van Vleck-Weisskopf	[24], [10]
	(8c)	0.012	1.05	1.4	2.04	FL = GR	full Lorentz or Gross	[24]
	(8d)	0.064	1.05	1.2	1.17	SL	single Lorentz	(10)
	(8e)	0.11	1.1	1.2	1.10	MVW	(VW) × ν_0/f	(Modified VW)
EXPERIMENT	(8f)	0.049	1	2.1	2.0	VW	for the local lines	[8], [11], Table II
	(8g)	0.061	1	2.1	1.22	GR		[29], [30]

as prescribed by a line shape function [24]. Five H_2O line bases, LB1 to 5, have been reported:

Line Base ID	LB1	LB2	LB3	LB4	LB5
Number of lines	38350	17201	2277	151	30 + α_c
Highest Frequency, THz	537	126	15	3	1
Remark	AFGL tape	revised AFGL	rotational spectrum	radio astronomy	EHF approximation
Reference	[25]	[26]	[27]	[28]	[10]

The low frequency wings of about 180 stronger (e.g., 6×10^4 dB/km at ν_0 = 2.64 THz, p = 101 kPa, v = 1 g/m^3, 300 K) air-broadened lines below 20 THz make a contribution in the EHF range [4]. For LB5, 30 local lines are formulated explicitly, and far-wing contributions from lines centered above 1 THz are fitted below 400 GHz to a continuum (slowly varying f-dependence) absorption

$$\alpha_c = k(p/101)v^x\theta^y(f/100)^z \quad \text{dB/km}. \tag{8}$$

A theoretical fit to (8) was accomplished on the basis of LB3 by subtracting the local lines below 1 THz from all 2277. Applying to each line five different standard shape functions led to the results summarized in Table III. Since the scale factor k varies over a wide range (e.g., 1:79 at 100 GHz), the obvious question is "which shape function is correct?" One criterion is the fact that integrated line absorption has to be finite. A shape function $F(f)$, normalized to unity at the line center frequency ν_0, should have a constant area $\pi\gamma$ (γ is line width) under the curve when f varies between 0 and ∞. A test can be defined by

$$\delta = \left[(1/\pi\gamma)\int_0^\infty F(f)\,df\right] - 1 = 0 \tag{9}$$

and used for checking the various line shapes. The most simple function is a single Lorentzian (SL) which in normalized form reads as

$$F_{SL} = a^2 b/[a^2 + (1-b)^2] \tag{10}$$

where $a = \gamma/\nu_0$ and $b = f/\nu_0$. Integration of (9) in closed form is not possible for all shape functions. A numerical integration over a limited range $b = 10^{-3}$ to 10^3 and $a = 0.001$ ($\nu_0 = 3000$, $\gamma = 3$ GHz) with five choices of $F(f)$ (see Table III and [36]) results in various amounts of deviation from (9):

$\delta = 0.0000$ (FL = GR), 0.0019 (SL), 0.0038 (MVW), 0.0082 (MGR), 0.64 (VW).

Although departures from (9) are caused predominantly by incorrect high frequency far-wing contributions, they also make the respective low frequency far-wing contributions suspect. Without getting involved in discussing merits of the various shape function, we note that only FL and GR oblige rigorously to (9). The MGR and VW shapes, based on (9) as well as other arguments, are not applicable to molecular line absorption over a wide spectrum range (0.01 to 20 THz) and their use for the water vapor spectrum should be discontinued [32]. More refined line shape treatments, possibly capable of predicting seven orders of magnitude in attenuation over many octaves require additional parameters [32]-[34] besides ν_0 and γ.

In fitting experimental water vapor EHF absorption, many workers applied the MGR-shape—with the result that large deficits were left unaccounted for and then labeled "excess" [4], [35]. The question whether the excess is a line shape problem or is caused by unaccounted absorbers (e.g., dimers and clusters of H_2O) has been a long-standing source for speculations in the correct modeling of water vapor attenuation [4], [7], [8], [11], [29], [35]. Equation (8) is, in the window ranges, the major (up to 85 percent at 100 GHz) contributor to α_V (7). The empirical continuum (8f), which was used in [8]-[11], provides too high an estimate for the scale factors c (Table II) and c_z (Table V) in ranges W3 and W4, leaving (8g) the better choice. This Rice-Ade continuum (see Table III) is supported by theory assuming the Lorentzian shape (10), that is (8g) $\cong$ (8d).

- Dry air attenuation mainly due to oxygen, can be estimated with the relation

$$\alpha_D = dp\theta^3 \quad \text{dB/km}. \tag{11}$$

Oxygen makes a small, though always present, contribution. The coefficient d (Table II) was calculated with the model detailed in [10]. The line-by-line summation includes overlap effects of the 60 GHz absorption band and nonresonant O_2 plus pressure-induced N_2 absorption.

- Smoke and suspended dust do not pose serious EHF attenuation problems [20]. A visibility in smoke of $U \cong 0.2$ km or a suspended mass concentration (dust) of 0.01 g/m^3 exhibit specific attenuations on the order of 0.15, 0.5, 1, and 3 dB/km in W1 to W4, respectively.
- In summary, the dominant role of H_2O in influencing atmospheric transparency (1) for terrestrial applications is evident. Concentrations of the various phase states are highly variable. Rain presents the most serious limitation to system performance. Assessing individual contributions to specific attenuation in (3) is difficult from measurements of A. Reliability, precision, and scale of supporting data (4) compromise the quality of most observations. Progress lies more in controlled laboratory experiments, where it is possible to study elements (except rain) of the accounting sum (3) in isolation.

Specific attenuations due to H_2O, (5) to (8), increase with frequency; also, temperature plays a role. At 220 GHz, the effectiveness to absorb has increased with reference to 35 GHz by different factors $\eta = [\alpha(220)/\alpha(35)]_i$:

Absorber i	Rain	Snow	Suspended Hydrometeor	Moist air
η	5	10	16	24

IV. RADIO PATH ATTENUATION

Attenuation (3) is evaluated from ($p\theta v + w + R$) distributions along a radio path. For a short horizontal path a set of average conditions (4) can be assumed and specific attenuations are simply multiplied by the geometric path length L.

The cumulative attenuation of a zenith radio path requires height profiles of $p - \theta - v$, w, and R as prescribed by *in situ* data or by a synthetic atmosphere (two-dimensional model). Liquid water content W, total precipitable water vapor V, rain cell depth L_R [15]-[18], and dry air attenuation d_z determine zenith attenuation which is modeled by [36]

$$A_z = \alpha_R L_R + b_z W + c_z V + d_z \quad \text{dB}, \tag{12}$$

where the water and vapor column densities are

$$W = \int_0^\infty w(h)\,dh \quad \text{and} \quad V = \int_0^\infty v(h)\,dh \quad \text{mm}. \tag{13}$$

Both quantities W and V can be measured simultaneously with a ground-based microwave radiometer over time scales from minutes to months [38], [39]. The coefficients b_z, c_z, and d_z have been evaluated for arctic, standard, and subtropical atmospheres specified in Table IV. Excess radio path length L_E due to refractive delay provides additional information about the air mass; dispersive effects from molecular resonances [10] are neglected. Results of three sets of air-mass-specific coefficients are listed in Table V. The example of A_z in Fig. 4 is for the U. S. Standard Atmosphere [37]. Calculation of A_z was performed "layer-by-layer" in a spherically stratified atmosphere encompassing 48 slabs between $h = 0$ and 30 km. The ratio b_z/c_z demonstrates the contribution of suspended hydrometeors to window absorption, relative to water vapor.

Slanted radio paths in clear air with an elevation angle $\phi \geq 6^\circ$ against horizontal follow a secant law [40]; i.e.,

$$A_\phi = A_z/\sin\phi \quad \text{dB}. \tag{14}$$

For modeling through rain, clouds, and low angle situations see [2], [15]-[17], [45].

V. CONCLUSION

Atmospheric EHF attenuation is a function of the radio path absorber population subject to considerable variations. Modeling runs the gamut from meteorological observables, through specific attenuations, to theoretical and experimental aspects of window transparencies. Results from a wide spectrum of recent work have been reviewed. Intricate "molecule-by-molecule," "line-by-line," "drop-by-drop" and "layer-by-layer" calculation procedures have been reduced to simple expressions allowing rapid estimations of window transparencies. No attempt was made to cover all possible angles of the subject matter. Rather, a direct line of thought was followed in order to convey some understanding of atmospheric EHF attenu-

TABLE IV
SELECTED PROPERTIES OF THREE MODEL ATMOSPHERES

MODEL ATMOSPHERE [37]	ID	PATH MEDIUM	H_2O SEA LEVEL $w(h=0)$	H_2O TOTAL (RH=100%) V,W	AVERAGE TEMPERATURE $\bar{T}^*$	REFRACTIVITY $N_0(h=0)$	REFRACTIVITY $N(h=30)$	EXCESS PATH LENGTH L_E^*
			g/m^3	mm	K	ppm	ppm	m
Arctic	1	Dry	0	0	224	316.0	3.4	2.287
U.S.Std	2	Air	0	0	243	273.1	4.1	2.283
Subtrop.	3	Mass	0	0	259	261.4	4.3	2.292
	1	Water	0.764	2.90	252	5.5	0	0.022
	2	Vapor	12.8	28.7	285	81.0	0	0.190
	3	V	27.2	70.4	288	164.9	0	0.447
	1	Cloud	-	0.100	252			
	2	Water	-	1.175	282			
	3	W	-	0.600	277			

$^*L_E = 10^6 \int_0^{30\ km} N(h)dh$

TABLE V
COEFFICIENTS b_z, c_z, AND d_z FOR CALCULATING ZENITH ATTENUATION A_z IN EHF WINDOW RANGES (SEE FIG. 4) FOR MODEL ATMOSPHERES SPECIFIED IN TABLE IV

EHF Window	Center Frequency	Model Atmosphere ID	Prediction [10] b_z	Prediction [10] c_z	Prediction [10] d_z	Prediction [10] b_z/c_z	Experiments $\bar{c}_z$	Experiments $\bar{d}_z$	Reference
	GHz		dB/mm $\times 10^{-2}$		dB		dB/mm $\times 10^{-2}$	dB	
		Arctic 1	1.71	1.10	0.24	155			
W1	35	U.S. Standard 2	1.40	0.91	0.20	154	0.5(3)	0.16(2)	[4], [11]
		Subtropic 3	1.00	0.84	0.19	119			
		1	4.49	5.90	0.36	76			
W2	90	2	4.83	4.67	0.32	103	2.6(5)	0.30(15)	[4], [11]
		3	4.63	4.19	0.30	111			
				[30], [10]					
		1	5.41	14.6	0.19	37			
W3	140	2	6.58	10.8	0.17	61	9(2)	0.2(1)	[4], [11], [41]
		3	7.53	10.1	0.16	75			
		1	5.92	32.0	0.16	19			
W4	220	2	7.75	25.7	0.15	30	15(5)	0.1(1)	[4], [11], [41]
		3	10.3	23.3	0.14	44	24(11)		[30]

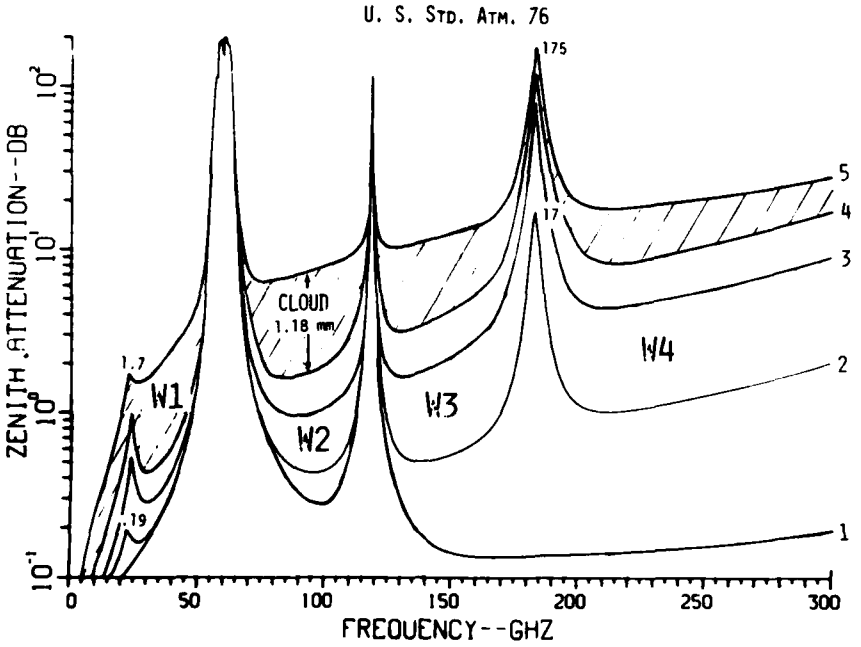

Fig. 4. One-way zenith attenuation A_z through the U.S. Standard Atmosphere [37] over the frequency range 5-300 GHz in 2.5 GHz steps for dry 1), moist 2), humid 3), and saturated air 4) and for 4) containing a rain-bearing cloud 5).

Curve ID	Delay L_E	Vapor V	Suspended Water W
	m	mm	mm
1	2.283	0	0
2	2.302	2.87	0
3	2.378	14.36	0
4	2.473	28.71	0
5	–	28.71	1.18

tion effects. The outcome of observations can be predicted, provided the physical variables (4) are available. In general, agreement with experimental data is within limits of their stated uncertainty (typically better than ± 15 percent). The theoretical basis for water vapor continuum absorption was discussed in more detail but still awaits confirmation of a correct and practical line shape function. Presently, the number and accuracy of experimental data decreases sharply above 100 GHz. There is a future in gathering more accurate data suitable to make adjustments to the proposed coefficient scheme.

ACKNOWLEDGMENT

The author wishes to thank K. C. Allen for the computer programming of rain and line shape models.

REFERENCES

[1] R. K. Crane, "Fundamental limitations caused by RF propagation," *Proc. IEEE*, vol. 69, no. 2, pp. 196–209, Feb. 1981.

[2] L. J. Ippolito, "Radio propagation for space communication systems," *Proc. IEEE*, vol. 69, no. 6, pp. 697–727, June 1981.

[3] L. J. Ippolito, R. K. Kaul, and R. G. Wallace, *Propagation Effects Handbook for Satellite Systems Design*, NASA Ref. Pub. 1082, 407 pages, 1981 (available from NASA Sci. Tech. Inform. Branch).

[4] H. J. Liebe, "Atmospheric water vapor: A nemesis for millimeter wave propagation," in *Atmospheric Water Vapor*, A. Deepak, T. Wilkerson, and L. Ruhnke, Eds. New York: Academic, 1980, pp. 143–201.

[5] D. C. Hogg, "Ground-based measurements of microwave absorption by tropospheric water vapor," in *Atmospheric Water Vapor*, A. Deepak, T. Wilkerson, and L. Ruhnke, Eds. New York: Academic, 1980, pp. 219–228.

[6] J. Preissner, "Einfluss der Atmosphaere auf mikrowellenradiometrische Messungen im Frequenzbereich von 10 GHz bis 400 GHz (atmospheric influence on radiometric measurements in the frequency range 10 to 400 GHz)," *DFVLR-Mitteilung 80-16*, Wissenschaftliches Berichtswesen, Deutsche Forschung-und Versuchsanstalt fuer Luft-und Raumfahrt, Cologne, West Germany, Sept. 1980. (Engl. translation: ESA Rep. TT-706, Aug. 1981.)

[7] S. M. Kulpa and S. A. Brown, Editors, "Near-millimeter wave technology base study, vol. I: Propagation," U.S. Army MDRC Rep. HD-SR-79-8, Nov. 1979, U.S. Govt. Printing Office 304-767 (DDC No. AD A079620).

[8] J. W. Waters, "Absorption and emission by atmospheric gases," in *Methods of Experimental Physics*, vol. 12B, ch. 2.3, M. L. Meeks, Ed., New York: Academic, 1976.

[9] E. K. Smith and J. W. Waters, "Microwave attenuation and brightness temperature due to the gaseous atmosphere," JPL Pub., 81-81, Jet Propulsion Lab., NASA, Pasadena, CA, Aug. 1981.

[10] H. J. Liebe, "Modeling attenuation and phase of radio waves in air at frequencies below 1000 GHz," *Radio Sci.*, vol. 16, no. 6, pp. 1183–1199, Nov.–Dec. 1981. (Also see K. C. Allen and H. J. Liebe, "Tropospheric absorption and dispersion of millimeter and submillimeter waves," *IEEE Trans. Antennas Propagat.*, vol. AP-31, no. 1, pp. 221–223, Jan. 1983.)

[11] R. K. Crane, "Attenuation estimates for the millimeter wave windows near 94, 140, 220 GHz," *ERT Doc. P-A502*, Environ. Res. Technol. Inc., Concord, MA, May 1980.

[12] D. Deirmendjian, "Far infrared and submillimeter wave attenuation by clouds and rain," Rand Corp. Re. AD-A021-947, Apr. 1975.

[13] R. L. Olsen, D. V. Rogers, and D. B. Hodge, "The aR^b relation in the calculation of rain attenuation," *IEEE Trans. Antennas Propagat.*, vol. AP-26, no. 2, pp. 318–329, Mar. 1978.

[14] V. C. Falcone, Jr., L. W. Abreu, and E. P. Shettle, "Atmospheric attenuation of millimeter and submillimeter waves: models and computer code," AFGL Environ. Res. Paper 679, U.S. Air Force Geophysics Lab., Hanscom AFB, MA, Oct. 1979.

[15] S. H. Lin, "Empirical rain attenuation model for earth-satellite

paths," IEEE Trans. Commun., vol. COM-27, pp. 812–817. May 1979.

[16] S. H. Lin, H. J. Bergmann, and M. V. Porsley, "Rain attenuation on earth-satellite paths—summary of 10 year experiments and studies," *Bell Syst. Tech. J.*, vol. 59, no. 2, pp. 183–228, 1980.

[17] K. Morita, "Estimation methods for propagation characteristics on earth-satellite links in microwave and millimeter wavebands," *Rev. Electr. Com. Lab. NTT*, vol. 28, no. 5, 6, pp. 459–471, 1980.

[18] R. K. Crane, "Prediction of attenuation by rain," *IEEE Trans. Commun.*, vol. COM-28, pp. 1717–1733, Sept. 1980.

[19] J. Nemarich, R. J. Wellman, D. Rocha, and G. B. Wetzel, "Characteristics of near-millimeter wave propagation in snow," *Proc. SPIE*, vol. 305, (Atmospheric Effects on EO, IR, and MMW System Performance) pp. 261–267, Aug. 1981.

[20] H. B. Wallace, "Millimeter-wave propagation measurements at the Ballistic Research Laboratory," *Proc SPIE*, vol. 305, pp. 224–231, Aug. 1981.

[21] H. R. Carlon, "Infrared water vapor continuum absorption: Equilibria of ions and neutral water clusters," *Appl. Opt.*, vol. 20, no. 8, pp. 1316–1322, 1981.

[22] B. Nilsson, "Meteorological influence on aerosol extinction in the 0.2-40 μm wavelength range," *Appl. Opt.*, vol. 18, no. 20, pp. 3457–3473, Oct. 1979.

[23] D. C. Hogg, F. O. Guiraud, and W. B. Sweezey, "The short-term temporal spectrum of precipitable water vapor," *Sci.*, vol. 213, pp. 1112–1113, Sept. 1981.

[24] A. J. Kemp, "Line shape functions for the computation of the absorption coefficient of water vapour at submillimetre wavelengths," *Infrared Phys.*, vol. 19, pp. 595–598, 1979.

[25] L. S. Rothman, "AFGL atmospheric absorption line parameters compilation: 1980 version," *Appl. Opt.*, vol. 20, no. 5 pp. 791–795, 1981.

[26] J. M. Flaud, C. Camy-Peyret, and R. A. Toth, "*Water Vapor Line Parameters from Microwave to Medium Infrared*," Oxford, England: Pergamon, 1981.

[27] M. Mizushima, "Absorption of millimeter to submillimeter waves by atmospheric water molecules," *Int. J. Infrared Millimeter Waves*, vol. 3, no. 3 pp. 379–384, 1982.

[28] R. L. Poynter and H. M. Pickett, "Submillimeter, millimeter, and microwave spectral line catalogue," JPL Pub. 80-23, Rev. 1, Jet Propulsion Lab., NASA, Pasadena, CA, June 1981.

[29] D. P. Rice and P. A. Ade, "Absolute measurements of the atmospheric transparency at short millimetre wavelengths," *Infrared Phys.*, vol. 12, pp. 575–584, 1979.

[30] C. C. Zammit and P. A. Ade, "Zenith atmospheric attenuation measurements at millimetre and sub-millimetre wavelengths," *Nature*, vol. 293, no. 5833, pp. 550–552, Oct. 1981.

[31] C. C. Zammit, R. E. Hill, and R. W. Baker, "Atmospheric emission and attenuation in the range 100 to 600 GHz measured from a mountain site," *Int. J. Infrar. Millimeter Waves*, vol. 3, no. 2, pp. 189–203, 1982.

[32] G. Birnbaum, "The shape of collision broadened lines from resonance to the far wings," *J. Quant. Spectro. Radiat. Transfer*, vol. 21, pp. 597–607, 1979.

[33] S. A. Clough, F. X. Kneizys, R. Davis, R. Gamache, and R. Tipping, "Theoretical line shape for H_2O vapor: Application to the continuum," in *Atmos. Water Vapor*, A. Deepak, T. Wilkerson, and L. Ruhnke, Eds., pp. 25–46, New York, Academic, 1980.

[34] M. E. Thomas and R. J. Nordstrom, "The N_2-broadened water vapor absorption line shape and infrared continuum absorption-II. Implementation of the line shape," *J. Quant. Spectrosc. Radiat. Transfer*, vol. 28, no. 2, pp. 103–112, 1982.

[35] R. J. Emery, A. M. Zavody, and H. A. Gebbie, "Measurements of atmospheric attenuation in the range 5-17 cm^{-1} and its temperature dependence," *J. Atmos. Terr. Phys.*, vol. 42, pp. 801–807, 1980.

[36] H. J. Liebe, "Millimeter wave properties of model atmospheres (1 to 300 GHz, 0 to 100 km)," *Nat. Telecom. Inform., Admin. Rep. Series*, to be published.

[37] NOAA, *U.S. Standard Atmosphere 1976*, National Oceanic and Atmospheric Administration Monograph NOAA-S/T 76-1562, U.S. Government Printing Office; and S. L. Valley, *Handbook of Geophysics and Space Environments*, ch. 2. New York: McGraw-Hill, 1965.

[38] F. O. Guiraud, J. Howard, and D. C. Hogg, "A dual-channel microwave radiometer for measurement of precipitable water vapor and liquid," *IEEE Trans. Geosci. Electron.*, vol. GE-17, no. 4, pp. 129–136, Oct. 1979.

[39] D. C. Hogg, F. O. Guiraud, J. B. Snider, M. T. Decker, and E. R. Westwater, "Microwave radiometry for measurement of water vapor," in *Reviews of Infrared and Millimeter Waves*, vol. 1, ch. 4. K. Button, Ed., New York: Plenum, 1982.

[40] E. E. Altshuler, M. A. Gallop, and L. E. Telford, "Atmospheric attenuation statistics at 15 and 35 GHz for very low elevation angles," *Radio Sci.*, vol. 13, no. 5, pp. 839–852, Sept.-Oct. 1978.

[41] V. F. Zabolotniy, I. A. Iskahakov, A. V. Sokolov, and E. V. Sukhonin, "Attenuation of radiation at wavelengths of 1.25 and 2.0 mm," *Infrared Phys.*, vol. 18, pp. 815–817, 1978.

[42] P. Misme and P. Waldteufel, "A model for attenuation by precipitation on a microwave earth-space link," *Radio Sci.*, vol. 15, no. 3, pp. 655–666, May-June 1980.

[43] E. J. Dutton, H. K. Kobayashi, and H. T. Dougherty, "An improved model for earth-space microwave attenuation distribution prediction," *Radio Sci.*, vol. 17, no. 6, pp. 1360–1370, Nov.-Dec. 1982.

[44] D. A. Stewart and O. M. Essenwanger, "A survey of fog and related optical propagation characteristics," *Rev. Geophys. Space Phys.*, vol. 20, no. 3, pp. 441–495, Aug. 1982.

[45] L. J. Ippolito, Ed., "NASA propagation experiments and studies," *Radio Sci.*, vol. 17, no. 6, pp. 1347–1520, Nov.-Dec. 1982.

Unclassified

SECURITY CLASSIFICATION OF THIS PAGE (When Data Entered)

AD-A127626

REPORT DOCUMENTATION PAGE

READ INSTRUCTIONS BEFORE COMPLETING FORM

1. REPORT NUMBER: 16638.14-GS	2. GOVT ACCESSION NO.: N/A
3. RECIPIENT'S CATALOG NUMBER: N/A	
4. TITLE (and Subtitle): Atmospheric EHF Window Transparencies Near 35, 90, 140, and 220 GHz	5. TYPE OF REPORT & PERIOD COVERED: Reprint
6. PERFORMING ORG. REPORT NUMBER: N/A	
7. AUTHOR(s): Hans J. Liebe	8. CONTRACT OR GRANT NUMBER(s): ARO 101-83
9. PERFORMING ORGANIZATION NAME AND ADDRESS: National Telecommunications and Information Administration, Boulder, CO 80303	10. PROGRAM ELEMENT, PROJECT, TASK AREA & WORK UNIT NUMBERS: N/A
11. CONTROLLING OFFICE NAME AND ADDRESS: U. S. Army Research Office, P. O. Box 12211, Research Triangle Park, NC 27709	12. REPORT DATE: Jan 83
	13. NUMBER OF PAGES: 9
14. MONITORING AGENCY NAME & ADDRESS(if different from Controlling Office)	15. SECURITY CLASS. (of this report): Unclassified
	15a. DECLASSIFICATION/DOWNGRADING SCHEDULE

16. DISTRIBUTION STATEMENT (of this Report)

Submitted for announcement only.

17. DISTRIBUTION STATEMENT (of the abstract entered in Block 20, if different from Report)

18. SUPPLEMENTARY NOTES

19. KEY WORDS (Continue on reverse side if necessary and identify by block number)

20. ABSTRACT (Continue on reverse side if necessary and identify by block number)

DD FORM 1 JAN 73 1473 EDITION OF 1 NOV 65 IS OBSOLETE

Unclassified

SECURITY CLASSIFICATION OF THIS PAGE (When Data Entered)